

Light-scattering study of the superconducting energy gap in $\text{YBa}_2\text{Cu}_3\text{O}_7$ single crystals

R. Hackl* and W. Gläser

Physik Department E21, Technische Universität München, D-8046 Garching, Federal Republic of Germany

P. Müller, D. Einzel, and K. Andres

Walther-Meißner-Institut für Tieftemperaturforschung, D-8046 Garching, Federal Republic of Germany

(Received 2 June 1988)

Raman scattering experiments have been performed on single-crystal samples of $\text{YBa}_2\text{Cu}_3\text{O}_7$ in order to investigate superconducting gap excitations. The electronic contribution to the total scattering intensity can be fitted well by a theoretical model of light scattering from quasiparticle pairs. Depending on the measuring symmetry, mean gap energies are found ranging from 3.0 to 5.5 $k_B T_c$.

The discovery of the new high- T_c superconductors^{1,2} has initiated unprecedented experimental and theoretical efforts in trying to understand the coupling mechanism.³ While pair correlations of charge carriers seems to follow from the observed quantum of flux⁴ ($\Phi_0 = h/2e$) and from Andreev scattering,⁵ experiments on the determination of the energy gap, 2Δ , still disagree widely. Δ may show considerable anisotropy, as was suggested from the beginning by both the structural and the superconducting properties of $\text{YBa}_2\text{Cu}_3\text{O}_7$. A recent tunneling study⁶ on single crystals reported gap values of 3.6 and 5.9 $k_B T_c$ for wave vectors parallel and perpendicular to the CuO a - b planes, respectively. As was shown first by Dierker, Klein, Webb, and Fisk in the $A15$ compounds,⁷ Raman scattering may be an alternative way to determine the gap structure.⁸ For polycrystalline samples^{9,10} and, very recently, for single crystals¹¹ of $\text{YBa}_2\text{Cu}_3\text{O}_7$, the opening of a gap has already been found by inelastic light scattering.

In this Rapid Communication, we report on Raman experiments on $\text{YBa}_2\text{Cu}_3\text{O}_7$ at temperatures above and below T_c . Single-crystal samples having different T_c are investigated at four scattering geometries. The data are analyzed quantitatively in terms of a broad distribution of gap energies.

The experiments were performed with standard Raman scattering equipment.⁸ The spectral resolution was set at 20 cm^{-1} . For excitation, the Ar^+ line at 458 nm was chosen. The penetration depth of light, δ , is estimated from optical data¹² to be about 700 Å. The exciting light, incident at an angle of approximately 65° to the surface normal, was focused to a spot of $0.08 \times 0.20 \text{ mm}^2$. The radiation-induced temperature increase in the spot ΔT was calculated from the thermal conductivity¹³ and the absorbed power ($P_a = 4mW$) and did not exceed 5 K near T_c and 15 K at 4.2 K. This estimate is in agreement with the observed Stokes to anti-Stokes ratio of two phonon lines. The samples were in a vacuum of better than 10^{-5} mbar and were mounted to the cold finger of a He-flow cryostat with adjustable temperature. To assure the reproducibility of the data, the samples were heated up to 200 K in periodic intervals in order to remove accumulating surface layers of adsorbed residual gas molecules. Four scattering geometries were investigated. The polar-

izations of the incident and the scattered light, E_i and E_s , had the following orientations with respect to the crystal axes: [100]-[100] (abbreviated below by 0°_{\parallel}), [100]-[010] (0°_{\perp}), [110]-[110] (45°_{\parallel}), and [110]-[1 $\bar{1}$ 0] (45°_{\perp}). On account of a - b twinning [100] and [010] were equivalent in the experiment.

The single crystals were grown from the flux as described in Ref. 14. Samples A and B were prepared in zirconia and alumina crucibles, respectively. The transition temperatures (midpoints) as determined by an eddy-current method, as well as by dc-magnetization measurements, were 88 K for sample A and 83 K for sample B . The transition widths were 0.5 and 20 K, respectively (see also Table I). Polarized-light microscopy showed a clearly visible domain structure originating from the a - b twinning of the orthorhombic crystals. The thickness of the sheetlike domains was typically 10 μm . The level of elastically scattered exciting light was very low. For frequency shifts larger than 50 cm^{-1} the discrimination was nearly complete.

Data of samples A and B taken at holder temperatures $T_h = 95$ K and $T_h = 4.2$ K are presented in Figs. 1(a)-1(d). All spectra above T_c consist of a smooth, almost flat, background and superimposed structures due to allowed and defect-induced scattering from phonons. For frequencies less than about 200 cm^{-1} , the scattering intensity at $T = 20$ K has decreased considerably below the one at 100 K without, however, vanishing towards $\omega = 0$. Between 200 and 600 cm^{-1} the superconducting intensity overshoots the one observed above T_c and asymptotically approaches the limit of the normal metal at higher energy transfers. In what follows, the discussion is focused on the nonvibronic part of the spectra. Since nearly all phonon structures depend only slightly on temperature, the vibronic scattering is easily separated out at 100 K and subtracted from all spectra measured above and below T_c . The phonon mode located near 340 cm^{-1} has to be subtracted separately on account of its anomalous temperature dependence. The remaining spectra, which are due to electronic scattering,¹¹ are divided by the almost constant one at 100 K, yielding a normalized cross section, $\sigma_{el}^0(\omega)$. The resulting 20-K spectra exhibit maxima at different, symmetry dependent frequencies and approach unity for

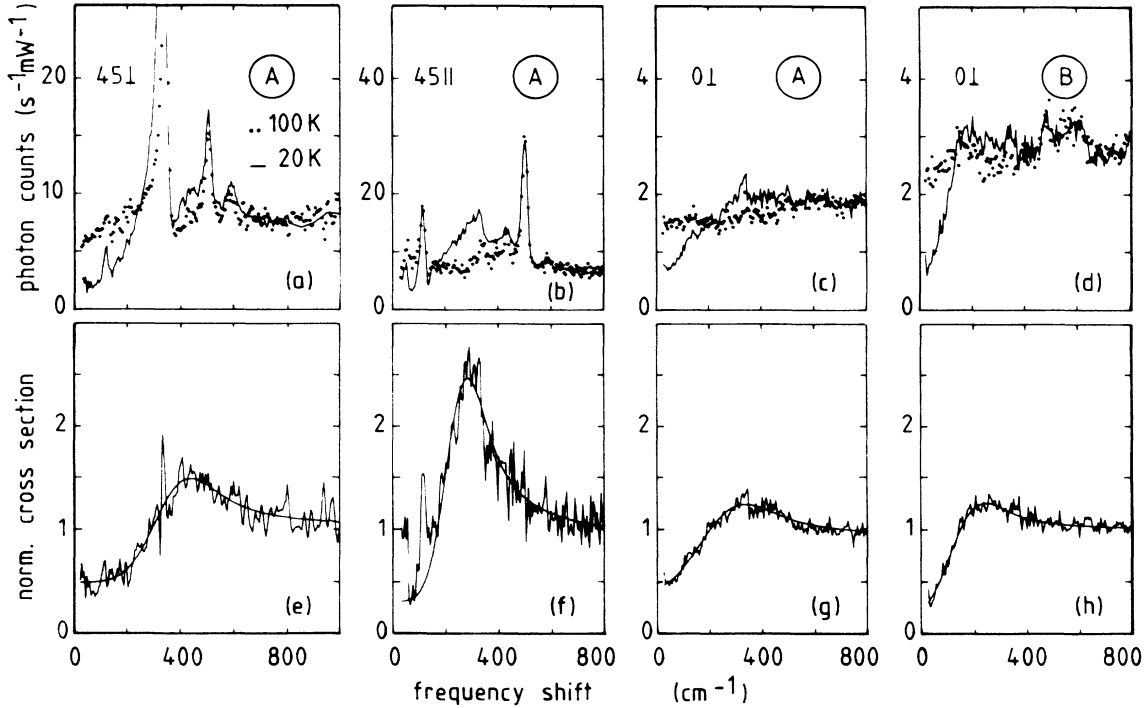


FIG. 1. (a)–(d) Raman spectra for single-crystal $\text{YBa}_2\text{Cu}_3\text{O}_7$ samples *A* and *B*. The temperatures relate to the illuminated spot. Symmetry assignments are indicated in the diagrams. (e)–(h) Normalized electronic scattering cross section $\sigma_{el}^0(\omega)$ of the 20-K spectra (a)–(d). The narrow features superimposed on the slowly varying spectra are, at least partly, due to small frequency shifts of the subtracted phonon structures. The spike at 120 cm^{-1} in (f) results from the anomalous temperature dependence of the corresponding phonon mode (see Ref. 11). The smooth lines are least-square fits using the model described in the text.

high-energy transfers [Figs. 1(e)–1(h)]. Because of the slight frequency dependence of the 0_1^+ spectra at 100 K [Figs. 1(c) and 1(d)], the procedure described is an approximation leading to a constant high-energy limit and is used to simplify the numerical evaluation. When the temperature is raised towards T_c , the amplitude of $\sigma_{el}^0(\omega)$ decreases, while the frequency of the peak structure shifts only slightly up to the highest measuring temperature of $0.95T_c$ (Fig. 2).

In the framework of present theories^{15,16} only a pair-breaking contribution to the weighted electronic structure function, $\tilde{S}(\mathbf{q}, \omega)$, can account for the intensity increase which is observed below T_c in the frequency range from 200 to 600 cm^{-1} . Since the superconducting coherence length is small compared to the optical penetration depth, $\xi \ll \delta$, the limit of small momentum transfer, q , holds. Thus, $\tilde{S}(\mathbf{q}, \omega)$ at $T=0$ varies as $(\Delta^2/\omega)(\omega^2 - 4\Delta^2)^{-1/2}$ for $\omega \geq 2\Delta$ as is derived from a conventional BCS model. The isotropic case has been generalized to allow for a \mathbf{k} dependence of Δ or, equivalently, for a distribution of gaps. The inelastic light scattering process projects out differently weighted gap distributions $P_s(\Delta)$, depending on the orientations of \mathbf{E}_i and \mathbf{E}_s . The normalized cross section at $T=0$ is given by^{7,16}

$$\sigma_{el}^0(\omega) = \int_0^{\omega/2} d\Delta P_s(\Delta) \left(\frac{\alpha \Delta^2}{\omega(\omega^2 - 4\Delta^2)^{1/2}} + 1 \right).$$

Constants and light scattering matrix elements are collected in the factor α , which like $P_s(\Delta)$ is determined by the measuring polarizations. The additive constant 1 ac-

counts for the experimentally observed difference between the low- and high-frequency end of the spectra and may be assigned to electronic interband transitions.^{7,11} The integration of this term leads to a low-frequency cutoff at $\omega = 2\Delta$ which is broadened by $P_s(\Delta)$. Since the interband scattering is found to be almost constant at 100 K, a considerable frequency dependence is expected at 20 K on account of the Bose-Einstein factor $[1 + n(T, \omega)]$. The effect, however, has been proven to be negligible due to cutoff energies exceeding $3k_B T_c$. The smooth lines in

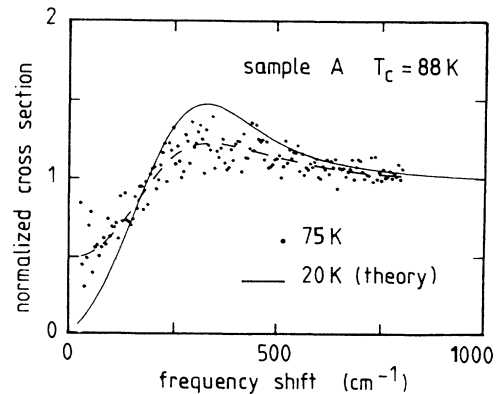


FIG. 2. Normalized electronic spectrum at 75 K. The symmetry is 0_1^+ . The solid line is the least-square-fit curve of Fig. 1(g). The broken line is only a guide to the eye. All spectra have been corrected for an energy independent background (see text).

Figs. 1(e)–1(h) represent the best fits using a Gaussian distribution of Δ and accounting for an additional energy independent background which is not given in the equation (compare Fig. 1 to Figs. 2 and 3). The background corrected normalized fits to all electronic spectra are illustrated in Fig. 3. In any case, the agreement with the data is striking [see Figs. 1(e)–1(g)]. Table I gives the numerical values found for samples *A* and *B*. The low-frequency end of the spectra near T_c is reminiscent of the temperature dependence of the thermal quasiparticle contribution to $\tilde{S}(\mathbf{q}, \omega)$ for large q (Ref. 17) (see Fig. 2). For finite q a theoretical investigation of the entire, finite temperature spectra has not yet been attempted (see Refs. 16 and 17).

Independent of details of the theoretical model which the fits are based on, the light scattering study clearly shows the existence of a gap in the electronic excitation spectrum. Furthermore, an anisotropy of the peak structures observed at different symmetries is seen explicitly. If the BCS description with a Gaussian distribution of Δ is a reasonable model, the mean gap energy found at 0°_\perp is $3.0k_B T_c$, while it is as large as $5.5k_B T_c$ for the 45°_\perp polarization. With a statistical weight of 15%, gap values exceeding $7.0k_B T_c$ may be deduced from this spectrum on the basis of the fitting procedure. The relative width σ/Δ_0 at the 0°_\perp symmetry is as large as 70% in both samples *A* and *B* (see Table I). The spectra observed at 45°_\parallel and 45°_\perp exhibiting an anisotropy of only 30% indicate that the broad structures of the two other symmetries are mainly due to intrinsic properties of $\text{YBa}_2\text{Cu}_3\text{O}_7$. Therefore, very small gaps should also be present. In addition, the finite slope of the theoretical fit curves at $\omega=0$ suggests the occurrence of vanishing gaps for some \mathbf{k} -space directions.

There is no direct relation between the gap energies found in the Raman experiment and certain directions in momentum space on account of the particular light-scattering process. Moreover, due to the orthorhombic structure of $\text{YBa}_2\text{Cu}_3\text{O}_7$, an unequivocal assignment of space-group symmetries to the respective polarizations of the incident and the scattered light is impossible. The tunneling data,⁶ however, indicate that the smaller value of the gap corresponds to a \mathbf{k} direction parallel to the c axis and the larger one to the a or b direction. The two gap energies, 3.6 and $5.9 k_B T_c$, observed by tunneling are approximately equal to the extremal mean values found in our experiment (see Table I). Surprisingly, the gap value assigned to $\mathbf{k}\parallel c$ is possibly seen at the a - b plane, where all photons are polarized perpendicular to the c axis. Howev-

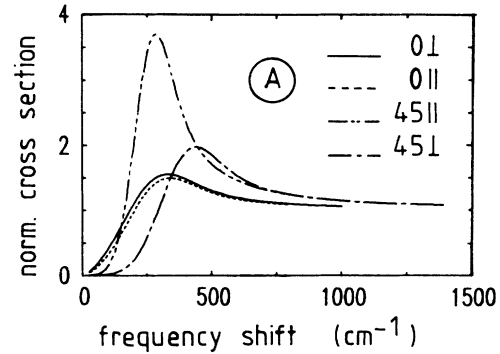


FIG. 3. Electronic scattering found at different symmetries (theoretical fits). The experimental points are omitted for clarity.

er, there may also be a large a - b anisotropy, which is concealed in the twinned crystals.

Because of the broad structures the temperature dependence of the gap energy cannot be derived directly from the data. The nearly constant maximum frequency (cf. Fig. 2), however, suggests a possible deviation from the BCS prediction as is also found by other methods.¹⁸ The gap structure, which is present in the spectra up to approximately $85 \text{ K} \approx 0.95T_c$, indicates that a large percentage of the probed surface layer remains superconducting very close to T_c . Thus, the broad features are not due to sample inhomogeneities, but can clearly be assigned to the anisotropy. Spectra measured between 40 and 80 K show that the probed surface layer of sample *B* remains superconducting only up to 65 K corresponding to the end point of the transition. Nevertheless, the relative width σ/Δ_0 is nearly unchanged (see Table I). In agreement with the tunneling study⁶ it appears that the anisotropy does not depend on the transition temperature.

In conclusion, the Raman experiments reveal clear evidence for the existence of a gap in the electronic excitation spectrum of $\text{YBa}_2\text{Cu}_3\text{O}_7$ up to $T/T_c = 0.95$. The observed broad structures are assigned to a large gap anisotropy showing up in the Raman spectra as symmetry dependent distributions of Δ . The mean gap energies range from 3.0 to $5.5 k_B T_c$. Additionally, the large distribution widths suggest gap energies in excess of $7k_B T_c$ as well as gaps which are very small if not zero for certain directions in \mathbf{k} space.

TABLE I. Symmetry-dependent mean gap energies $2\Delta_0$ of $\text{YBa}_2\text{Cu}_3\text{O}_7$. σ^2 is the variance of the Gaussian assumed for the gap distribution. The highest temperature, where the Raman spectrum of sample *B* exhibits a gap structure, was 60 K. Thus, $T_c = 65 \text{ K}$ was used to calculate $2(\Delta_0 \pm \sigma)/k_B T_c$.

Sample	T_c (K)	Polarizations	$\Delta_0 \pm \sigma$ (cm^{-1})	$\frac{\sigma}{\Delta_0}$ (%)	$\frac{2(\Delta_0 \pm \sigma)}{k_B T_c}$
<i>A</i>	88	0°_\perp	91 ± 61	67	3.0 ± 2.0
		0°_\parallel	98 ± 56	57	3.2 ± 1.8
		45°_\parallel	113 ± 32	28	3.7 ± 1.0
		45°_\perp	169 ± 48	28	5.5 ± 1.6
<i>B</i>	83	0°_\perp	60 ± 44	73	2.6 ± 1.9

The assistance of J. Sedlmeir and C. Rausch during the numerical evaluation of the data is gratefully acknowledged. The work has partly been supported by the Bundesministerium für Forschung und Technologie.

*Present address: Walther-Meissner für Tieftemperaturforschung, D-8046 Garching, Federal Republic of Germany.

¹J. G. Bednorz and K. A. Müller, *Z. Phys. B* **64**, 189 (1986).

²M. K. Wu, J. R. Ashburn, C. J. Torng, P. H. Hor, R. L. Meng, L. Gao, Z. J. Huang, Y. Q. Wang, and C. W. Chu, *Phys. Rev. Lett.* **58**, 908 (1987).

³For references see, e.g., *Proceedings of the International Conference on High- T_c Superconductors and Materials and Mechanisms of Superconductivity, Interlaken, Switzerland, 1988*, edited by J. Müller and J. L. Olsen [*Physica C* **153-155**, (1988)].

⁴C. E. Gough, M. S. Colclough, E. M. Forgan, R. G. Jordan, M. Keene, C. M. Muirhead, A. I. M. Rae, N. Thomas, J. S. Abell, and S. Sutton, *Nature* **326**, 855 (1987).

⁵H. F. C. Hoevers, P. J. M. van Bentum, L. E. C. van de Leemput, H. van Kempen, A. J. G. Schellingerhout, and D. van der Marel, *Physica C* **152**, 105 (1988).

⁶J. S. Tsai, I. Takeuchi, J. Fujita, T. Yoshitake, S. Miura, S. Tanaka, T. Terashima, Y. Bando, K. Iijima, and K. Yamamoto, in Ref. 3, p. 1385.

⁷S. B. Dierker, M. V. Klein, G. W. Webb, and Z. Fisk, *Phys. Rev. Lett.* **50**, 853 (1983).

⁸R. Hackl, Doctoral thesis, Technische Universität München,

1987 (unpublished).

⁹Yu. A. Ossipyan, V. B. Timofeev, and I. F. Shegolev, in Ref. 3, p. 1133.

¹⁰K. B. Lyons, S. H. Liou, M. Hong, H. S. Chen, J. Kwo, and T. J. Negran, *Phys. Rev. B* **36**, 5592 (1987).

¹¹S. L. Cooper, M. V. Klein, B. G. Pazol, J. P. Rice, and D. M. Ginsberg, *Phys. Rev. B* **37**, 5920 (1988).

¹²J. Humlicek, M. Garriga, M. Cardona, B. Gegenheimer, E. Schönherr, P. Berberich, and J. Tate, *Solid State Commun.* **66**, 1071 (1988).

¹³U. Gottwick, R. Held, G. Sparn, F. Steglich, H. Rietschel, D. Ewert, B. Renker, W. Bauhofer, S. von Molnar, M. Wilhelm, and H. E. Hoinig, *Europhys. Lett.* **4**, 1183 (1987).

¹⁴P. Müller, K. Andres, F. Gross, H. Veith, and R. Hackl, in Ref. 3, p. 421, and references therein.

¹⁵A. A. Abrikosov and L. A. Fal'kovskii, *Zh. Eksp. Teor. Fiz.* **40**, 262 (1961) [*Sov. Phys. JETP* **13**, 179 (1961)].

¹⁶M. V. Klein and S. B. Dierker, *Phys. Rev. B* **29**, 4976 (1984).

¹⁷D. R. Tilley, *Z. Phys.* **254**, 71 (1972).

¹⁸A. Wittlin, L. Genzel, M. Cardona, M. Bauer, W. König, E. García, M. Barahona, and M. V. Cabañas, *Phys. Rev. B* **37**, 652 (1988).